Nuclear deformations of ^{24}Mg, ^{28}Si, and ^{32}S from fast neutron scattering

G. Haouat, Ch. Lagrange, R. de Swiniarski,* F. Dietrich,† J. P. Delaroche, and Y. Patin
Centre d'Etudes de Bruyères-le-Châtel, Service de Physique Neutronique et Nucléaire, 91680 Bruyères-le-Châtel, France
(Received 17 July 1984)

Nuclear deformation of the s-d shell nuclei ^{24}Mg, ^{28}Si, and ^{32}S has been investigated by means of fast neutron scattering. Differential cross sections have been measured at the incident neutron energies of 9.76 and 14.83 MeV, over the angular range from 15° to 160°. Angular distributions have been obtained for the elastic scattering and the inelastic scattering to low lying collective states. The measurements have been compared to the predictions of collective models, and nuclear deformations have been determined for these nuclei. The coupled-channel and compound-nucleus formalisms were used in the calculations. The analysis shows that these nuclei exhibit quite different shapes, and confirms the oblate deformation of ^{28}Si established in recent works. A detailed comparison of the deformations obtained in this study with those deduced from (p,p'), (d,d'), (α,α'), (^{16}O, ^{16}O'), other (n,n'), and charge distribution measurements is presented and discussed. It is emphasized that for these $N=Z$ nuclei the quadrupole deformations and deformation lengths are in very good agreement when measured through neutron and proton scattering as well as electromagnetic excitations.

I. INTRODUCTION

It is generally accepted that nuclei in the $2s$-$1d$ shell mass region exhibit a collective behavior. This is especially true for nuclei at the beginning of this shell since both rotational levels and large static quadrupole moments are firmly established from many measurements.[1] Moreover, the results of Hartree-Fock (HF) type of calculations characterize the s-d shell as a region of permanent ground-state deformation.[2] Some of these calculations suggest that nuclei in this region have ground-state quadrupole and hexadecapole deformations which change both in magnitude and sign through the shell.[3]

The most extensive and accurate data on nuclear deformations have come traditionally from Coulomb excitation measurements. Such measurements provide only information on the charge distribution in nuclei. Deformations of the mass (or nuclear potential) distribution have, however, been obtained through inelastic hadron scattering experiments. Measurements of multipole moments of the nuclear potential have been performed for deformed nuclei of the s-d shell[4–7] and rare-earth[8–11] regions as well as for several actinide nuclei.[12–18] The analysis of inelastic scattering cross sections is usually carried out through the deformed optical-model potential since the actual effective interaction is still poorly understood. The deformed optical model has, indeed, been extremely powerful, in particular for the determination of multipole moments of rare-earth nuclei.[8,19–21]

A large number of measurements have been performed on $4n$ s-d shell nuclei, using hadronic probes such as α particles,[5,22] helions,[23,24] polarized and unpolarized protons,[6,25] heavy ions,[26,27] and neutrons;[28–33] in the latter case, the studies were often limited to the determination of quadrupole deformations (β_2). Very large variations among different results are mainly observed for the hexadecapole deformation parameters (β_4). Differences are also observed with nuclear charge deformations. In general, small β_4 deformations have been obtained with composite particles (α, ^{3}He) while large β_4 values have been derived from proton or electron scattering measurements. Such large differences still remain after the various results are compared through the deformation lengths $\beta_\lambda R$ (R being the nuclear charge or potential radius and $\lambda=2,4$) instead of β_λ deformations.[34] They also persist through the multipole moments $q_{\lambda 0}$ of the nuclear charge or potential distribution, as pointed out by Mackintosh.[35] Coulomb excitation and inelastic electron scattering experiments reveal details only about the charge distribution in nuclei and determine, in fact, the charge deformation parameters β_2^C, β_4^C, ... On the other hand, strongly interacting particles like α, p, or neutrons are more sensitive to the whole nuclear potential; therefore, the β_2^N, β_4^N, . . . , values extracted from inelastic hadron scattering experiments may indeed be different from β_2^C,β_4^C values. Many explanations of these observed differences have been proposed: (i) the validity of the models used to describe the reaction mechanisms and the nuclear processes,[20] (ii) the difference between charge and mass (potential) distributions in nuclei,[11] and (iii) the dependence of the deformation parameters on the external probe through the excitation process of the nucleus.[36]

Discrepancies between the hexadecapole deformation parameters extracted from (α,α'), (^{3}He,^{3}He'), and (p,p') measurements on s-d shell nuclei have, however, been partly removed, in particular by Mackintosh,[37] and Rebel and Schweimer,[38] by using the deformed, collective folding model. Their calculations suggest that the deformation of the underlying nuclear matter distribution is much different from that of the phenomenological optical potential.

Although protons appear to have several advantages over composite particles as probes of nuclear shapes, as was suggested by Mackintosh,[39] neutrons have the additional advantage, as chargeless particles, of being sensitive only to the nuclear field. Since only a few experiments of

neutron inelastic scattering from s-d shell nuclei have been performed so far, with most of the time a poor energy resolution,[28–33] a new and accurate determination of these cross sections for some $4n$ s-d shell nuclei, ^{24}Mg, ^{28}Si, and ^{32}S, is desirable. In fact, the importance of precise knowledge of multipole deformations for the s-d nuclei was stressed in a recent experiment of inelastic scattering of 800 MeV polarized protons performed at Los Alamos.[40]

The measurement presented here was performed using the time-of-flight technique at two neutron energies, 9.76 and 14.83 MeV, with natural samples of Mg, Si, and S. Indeed, one of the goals of the experiment was to measure cross sections for low-lying 0^+, 2^+, and 4^+ states of ^{24}Mg, ^{28}Si, ^{32}S, and, possibly, for higher excited states in order to further check or determine nuclear shapes by means of deformation parameters extracted from coupled-channel analyses. Another goal of this experiment was to check some possible energy dependence of the deformation parameters as was surprisingly observed recently for ^{28}Si with protons in the energy range 14—40 MeV.[41] Moreover, although the oblate shape of ^{28}Si is now clearly established, in agreement with most theoretical works,[2,3] the precise shape of ^{24}Mg and mainly ^{32}S has still to be investigated. For instance, an experiment of 30 MeV polarized proton inelastic scattering from ^{32}S did not help to decide whether this nucleus has a prolate or oblate deformation.[6] A more recent 13.9 MeV neutron spin-flip probability measurement on ^{32}S (2^+) was also unable to distinguish clearly between the vibrational and the rotational character of this nucleus.[42]

In the following, we present, in Sec. II, the experimental apparatus used for the measurements and the data reduction method. The measured cross sections, for the low-lying states in the three nuclei at the two incident neutron energies, are discussed in Sec. III. Section IV describes the analysis of the measurements which takes into account the direct interaction mechanism, through the coupled-channel formalism, and the compound-nucleus process, by means of the Hauser-Feshbach statistical model. The extracted optical potential and deformation parameters are discussed in Sec. V and compared to those from other experimental and theoretical works. Conclusions are summarized in Sec. VI.

II. EXPERIMENTAL METHOD AND DATA REDUCTION

The differential cross sections were measured using the neutron time-of-flight facility of the Centre d'Etudes de Bruyères-le-Châtel tandem accelerator laboratory.[20] The experimental technique and the data acquisition and processing have been described extensively in Ref. 43; only brief details are given here.

Monoenergetic neutrons of 9.76 and 14.83 MeV were produced from the ^{2}H(d,n)^{3}He reaction. The EN tandem Van de Graaff accelerator delivered a deuteron beam pulsed at a repetition rate of 2.5 MHz and bunched into bursts with a time dispersion of 0.8—1.0 ns full width at half maximum; the average beam current was typically 2 μA. The deuterons were incident on a 3 cm long deuterium gas target filled at a pressure of 1.5 atm and separated from the evacuated beam line by a 3.5 mg/cm^2 thick nickel foil. The primary neutrons, with an energy spread of 170 keV at 9.76 MeV and 120 keV at 14.83 MeV, bombarded cylindrical samples located at 0° with respect to the deuteron beam axis and at 12 cm from the gas-target center. Natural samples of magnesium (79.0% ^{24}Mg, 10.0% ^{25}Mg, 11.0% ^{26}Mg), silicon (92.2% ^{28}Si, 4.7% ^{29}Si, 3.1% ^{30}Si), and sulfur (95.0% ^{32}S, 0.8% ^{33}S, 4.2% ^{34}S) were used for the measurements; they all had a diameter of 2.0 cm and masses of 23.9, 32.2, and 25.4 g, respectively. The relatively high isotopic purity of these samples means that the results presented here are mainly representative of the most abundant components, ^{24}Mg, ^{28}Si, and ^{32}S, respectively.

The scattered neutrons were detected by an array of five detectors separated from each other by 20°. The detectors consisted of 12.5 cm diam, 5-cm thick NE213 liquid scintillators optically coupled to XP-1041 photomultiplier tubes. Each detector was housed in a massive shield of paraffin loaded with lithium carbonate and borax. A set of five 1m long shadow bars, made of iron and tungsten, were placed around the scattering sample in order to intercept direct neutrons from the source in the detector direction. Intermediate 1.5- and 0.5-m long collimators of paraffin loaded with lithium carbonate and borax were placed between the detector shielding and the shadow

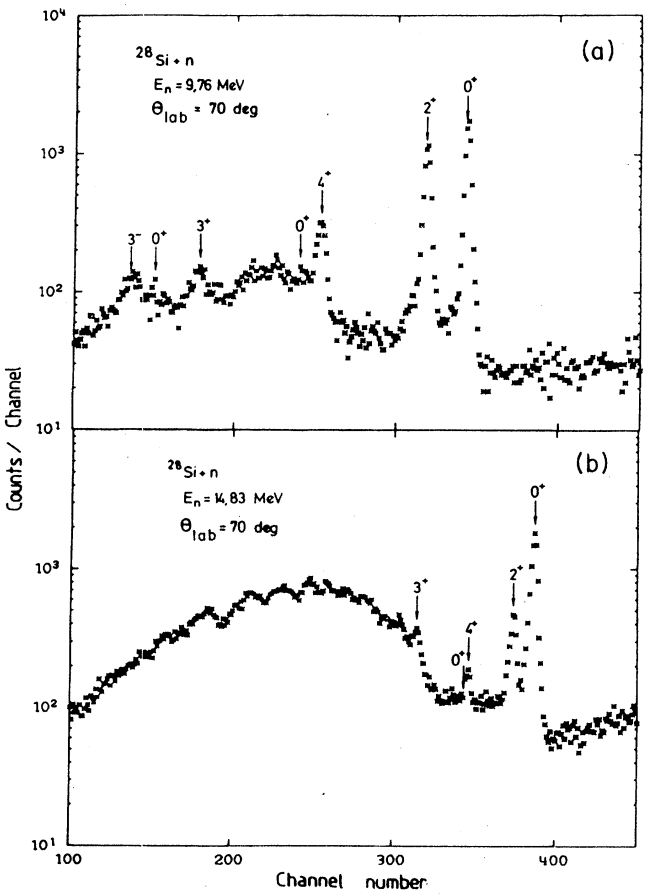

FIG. 1. Time-of-flight spectra for neutrons scattered by ^{28}Si at the energies of 9.76 MeV (a) and 14.83 MeV (b).

bars; they greatly reduced time-independent background in the scattered neutron spectra. The flight path from the sample to each detector was 8 m. The overall energy resolution of the spectrometer was $\simeq$200 keV at 9.76 MeV and $\simeq$300 keV at 14.83 MeV. These experimental conditions were sufficient to resolve in the time-of-flight spectra neutron groups from elastic scattering and inelastic scattering to the first excited states of ^{24}Mg, ^{28}Si, and ^{32}S. Time-of-flight spectra for 9.76 and 14.83 MeV neutrons scattered by silicon are shown in Fig. 1 to illustrate the experimental resolution and the good separation between the scattered neutron groups.

Data were taken using a standard electronic setup. Pulse shape discrimination was employed to reject most of the γ-ray-induced events in the scintillators. This greatly contributed to reducing time independent background in the time-of-flight spectra. For each detected neutron, the time-of-flight and the recoil-proton energy in the scintillator were recorded in a two-parameter mode.[16] The linear pulse height threshold could then be adjusted in off-line data processing to obtain a good compromise between the signal-to-background ratio and the statistical uncertainty in the yields extracted from the time-of-flight spectra.

Normalization of the data was obtained by measuring with the same detector the incident and scattered neutron fluxes; for the incident-flux measurement the detectors were placed at 0°, the scattering sample being removed. Thus, to deduce the absolute value of the cross sections, only values of the efficiency relative to that of the primary neutron energy were needed. The energy dependence of this relative efficiency was determined for each detector by comparing the yields of the neutron source at various angles with the corresponding cross sections for the ^{2}H(d,n)^{3}He reaction.[44]

The primary neutron flux was monitored continuously during the runs with an auxiliary detector, identical with the main detectors, which viewed directly the neutron source at a fixed angle of 55° and a distance of $\simeq$5 m. The time-of-flight and linear signals of the monitor detector were recorded together with the signals of the main detectors; with this arrangement deadtime differences were reduced to less than 0.5% and thus neglected.

Measurements were completed at 28 angles between 15° and 160° for each sample and at the two incident neutron energies. Sample-in and sample-out runs were taken. After the background subtraction was achieved, yields were obtained for isolated peaks in the time-of-flight spectra, both by direct summation of counts and by fitting line shapes to the peaks, to check for consistency of the yield extraction. For peaks too close to each other to be resolved completely, yields were obtained by an unfolding procedure using the line shapes deduced from the analysis of well-resolved peaks. The net yields were converted to differential cross sections after corrections for anisotropy of the incident neutron beam and finite size effects in the sample had been applied. These latter corrections included those for neutron flux attenuation by the sample, multiple scattering, and angular spread of the incident neutron trajectories; the corrections were calculated using an analytic method similar to that developed by Kinney.[45] No isotopic corrections were made, since neither the elastic yields nor the corresponding inelastic yields from the minor isotopes could be resolved from those of the major isotopes.

Uncertainties in the measurements include those affecting the reproducibility of the measured yields and those associated with the normalization of the data. The normalization uncertainties are small in the present experiment since the incident and scattered neutron fluxes were measured with the same detector, the main contributions originating with the determination of the energy dependence of the detector efficiency and with the corrections for sample-size effects; all together they comprise an uncertainty of about 6%. The reproducibility uncertainties arise from counting statistics, background substraction, unfolding procedures, dispersion in the monitor indications, and sample positioning. They combine to yield an uncertainty ranging from 2% to 10% for the elastic scattering cross sections and from 5% to 20% for the inelastic scattering cross sections presented here.

III. EXPERIMENTAL RESULTS

Angular distributions were obtained for the elastic scattering and inelastic scattering to levels of up to $\simeq$6 MeV excitation energy.[43] For levels of higher excitation energy, extraction of the yields was questionable, especially at 14.83 MeV incident energy, because the corresponding scattered neutron groups were superimposed, in the time-of-flight spectra, on a wide continuum. This continuum was generated mainly by elastic scattering, from the sample, of neutrons of the ^{2}H(d,np)^{2}H breakup reaction. Thus a reliable subtraction of the background from the yields was impossible to achieve.

The differential cross sections for elastic scattering from ^{24}Mg, ^{28}Si, and ^{32}S at 9.76 and 14.83 MeV are displayed in Fig. 2. The curves shown in this figure, and in subsequent figures, are theoretical fits to the data which will be discussed in Sec. IV. Several interesting features emerge from the observation of the experimental results. The 9.76 MeV cross sections decrease systematically in the angular range 70°—105° as one goes from ^{24}Mg to ^{32}S, and increase at angles beyond $\simeq$110°, although a third minimum appears at 150° in the angular distribution of ^{32}S [Fig. 2(a)]. A similar, but rather less pronounced, behavior is observed at 14.83 MeV [Fig. 2(b)]. These phenomenological features seem to be related to nuclear structure properties. Indeed, in a recent study of nuclear structure effects on 35.2 MeV proton scattering from light nuclei, Fabrici *et al.*[25] demonstrated a definite correlation between the elastic cross sections at backward angles and the quadrupole deformation parameters. These authors also showed that, for the inelastic scattering to the first 2^+ state, there is an enhanced backward yield resulting from nuclear deformation effects.[25] These effects are not apparent in our corresponding neutron cross sections displayed in Fig. 3. This is not too surprising since this backward angle effect shows up, in proton inelastic scattering, only at energy above 26 MeV.[25] Moreover, at the energies of the present neutron measurements, the contribution of the compound-nucleus mechanism to the first 2^+ state cross sections is still large, especially at 9.76

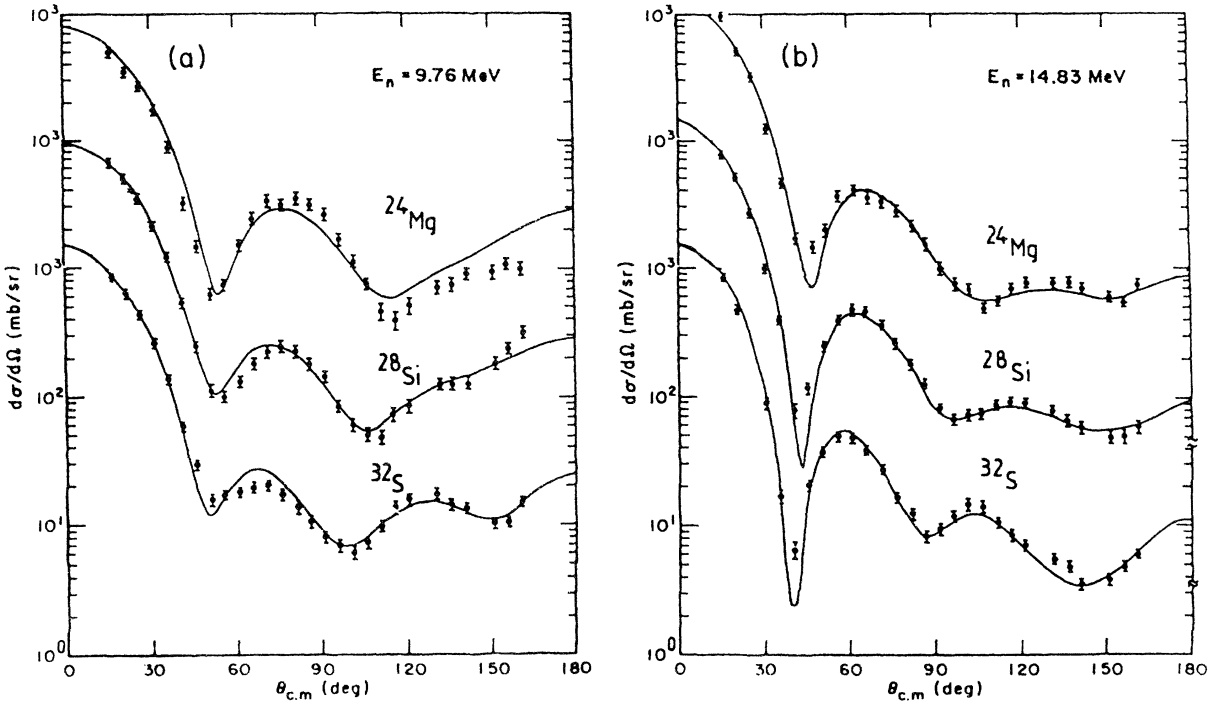

FIG. 2. Experimental neutron elastic scattering angular distributions for ^{24}Mg, ^{28}Si, and ^{32}S at 9.76 MeV (a) and 14.83 MeV (b). The curves correspond to coupled-channel calculations, assuming for the three nuclei the axially symmetric rotational model. The calculations include compound-nucleus and direct-interaction contributions.

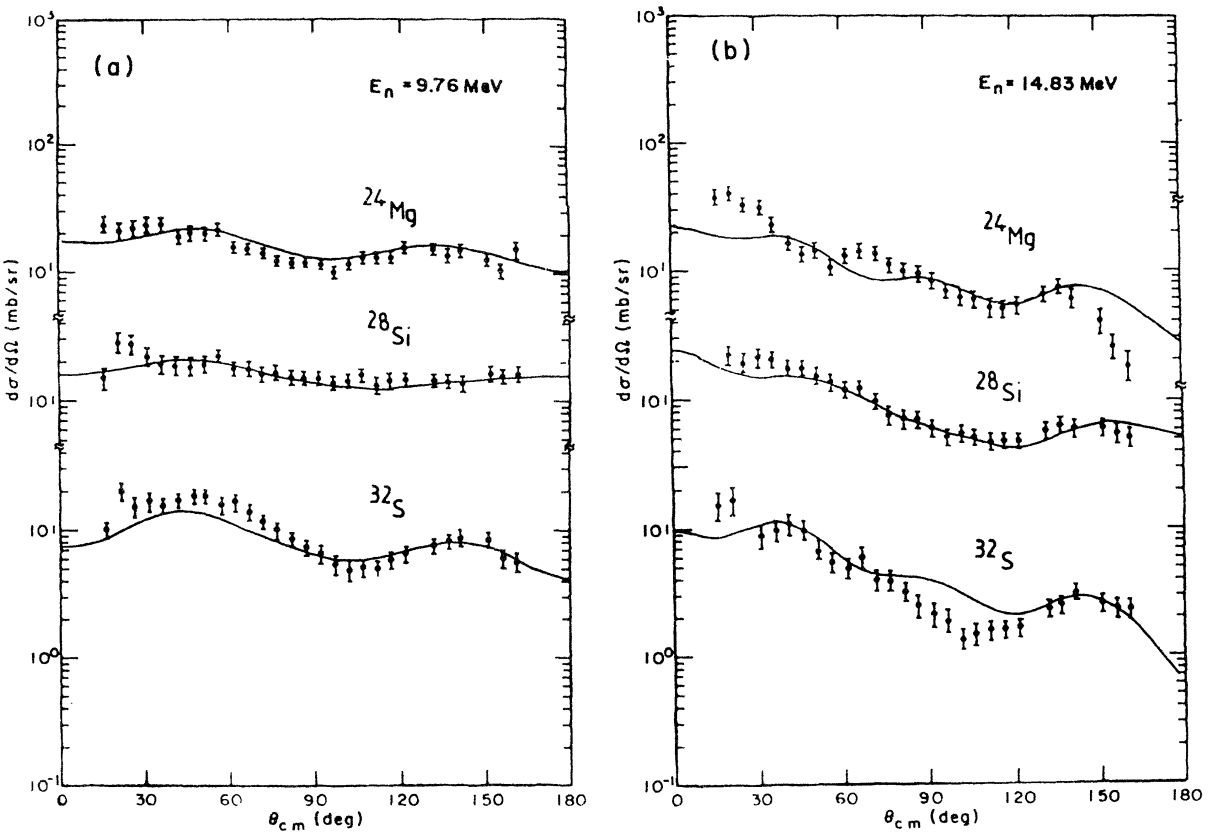

FIG. 3. Experimental neutron inelastic scattering angular distributions at 9.76 MeV (a) and 14.83 MeV (b) for the first 2^+ states in ^{24}Mg, ^{28}Si, and ^{32}S. The curves correspond to calculations including DI and CN contributions. The DI cross sections were calculated assuming the axially symmetric rotational model.

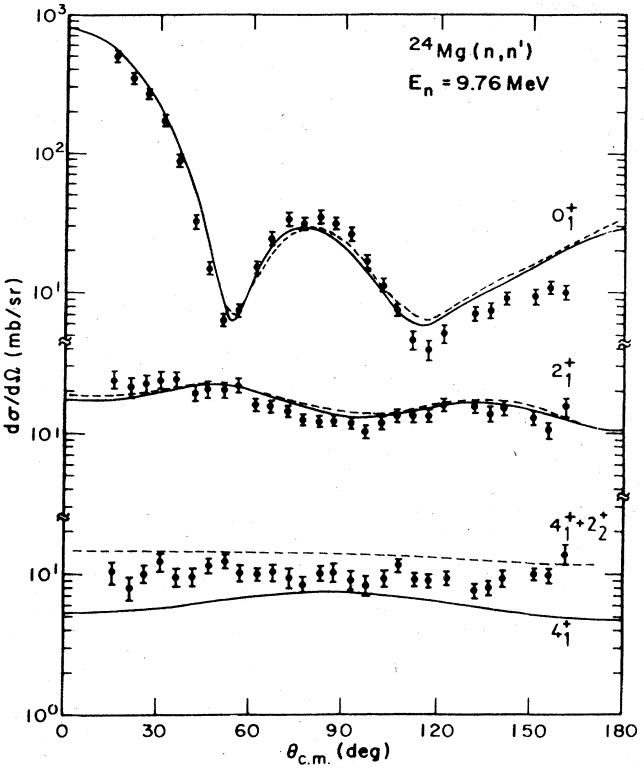

FIG. 4. Elastic and inelastic scattering differential cross sections at 9.76 MeV for ^{24}Mg. The full lines correspond to the symmetric rotor (S) calculations, the dashed lines to the asymmetric rotor (T) calculations.

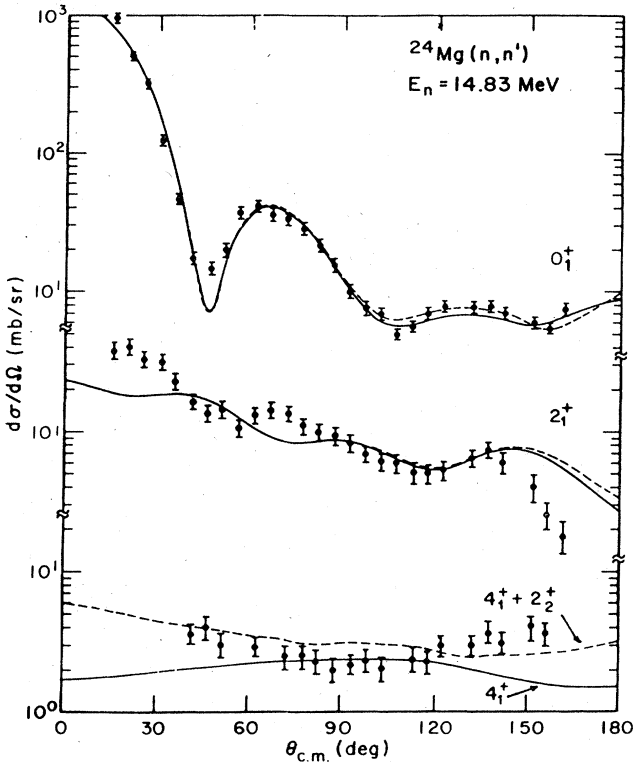

FIG. 5. Elastic and inelastic scattering differential cross sections at 14.83 MeV for ^{24}Mg. The full lines correspond to the symmetric rotor (S) calculations, the dashed lines to the asymmetric rotor (T) calculations.

MeV, and thus washes out possible deformation effects. Nevertheless, the systematic changes in the shape and magnitude of the angular distributions for the three nuclei (Fig. 3) are directly related to the nuclear deformations, as will be discussed in Sec. IV.

Since our experimental resolution was not good enough to separate the contributions of a number of high-energy excited states, we present in Figs. 4 and 5 the summed cross sections for the 4^+ (4.123 MeV) and 2^+ (4.239 MeV) states of ^{24}Mg obtained at 9.76 and 14.83 MeV, respectively. On the other hand, cross sections could be obtained at both energies for the 4^+ (4.618 MeV) state of ^{28}Si. These are displayed in Figs. 6 and 7. For ^{32}S, the cross sections for the 0^+ (3.779 MeV), 2^+ (4.282 MeV), and 4^+ (4.459 MeV) states could be obtained separately at 9.76 MeV; they are shown in Fig. 8. But we could not resolve the 2^+ (4.280 MeV), 4^+ (4.459 MeV), and 1^+ (4.695 MeV) states at 14.83 MeV; their summed cross sections are displayed in Fig. 9.

IV. DATA ANALYSIS

In this work the neutron energies have been chosen sufficiently high to expect that the deformation effects are predominant in the scattering cross sections. However, in order to obtain realistic values of the deformation parameters, the data have been analyzed assuming that the interaction mechanism involves an incoherent superposition of the direct interaction (DI) and compound nucleus (CN) processes; the former depends directly upon the structure of the nucleus, while the latter is nearly insensitive to nuclear structure.

The direct interaction cross sections were calculated using the coupled-channel formalism and a deformed neutron potential of the following form:

$$U=-Vf(r,R_v,a_v)+4ia_D W_D\frac{d}{dr}f(r,R_D,a_D)$$

$$+2\lambda_\pi^2 V_{SO}\vec{l}\cdot\vec{s}\,\frac{1}{r}\frac{d}{dr}f(r,R_{SO},a_{SO})\,. \quad (1)$$

No volume-absorption term is included here since its effect on the calculated cross sections is believed to be negligible at the energies of the present work. This assumption is strengthened by recent analyses of neutron scattering from light nuclei.[33,54] The form factor f is of a Woods-Saxon type

$$f(r,R_i,a_i)=\{1+\exp[(r-R_i)/a_i]\}^{-1}\,,$$

where R_i is a potential radius and a_i the corresponding diffusiveness. Only the real and surface-imaginary potentials were deformed, since the effects of deforming the spin-orbit potential on the calculated angular distributions

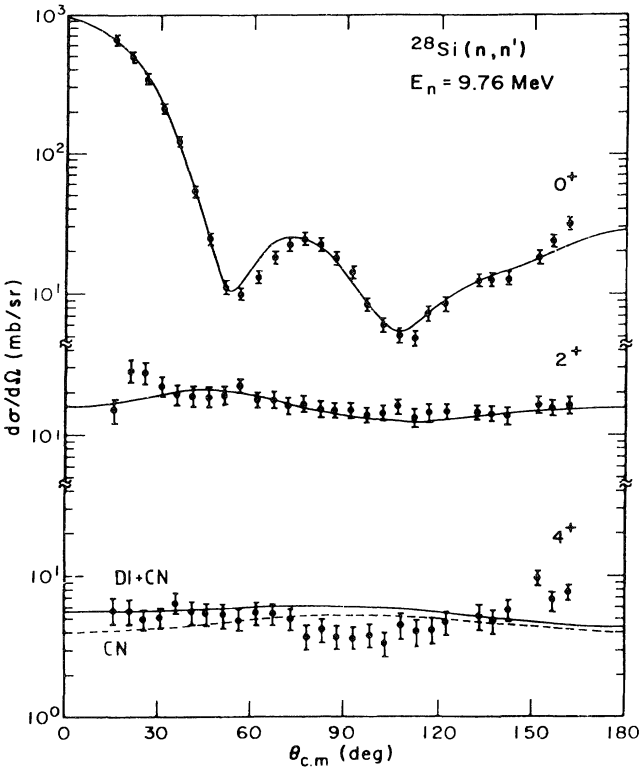

FIG. 6. Elastic and inelastic scattering differential cross sections at 9.76 MeV for ^{28}Si. The full lines correspond to calculations including DI and CN contributions. The dashed line corresponds to the CN contribution.

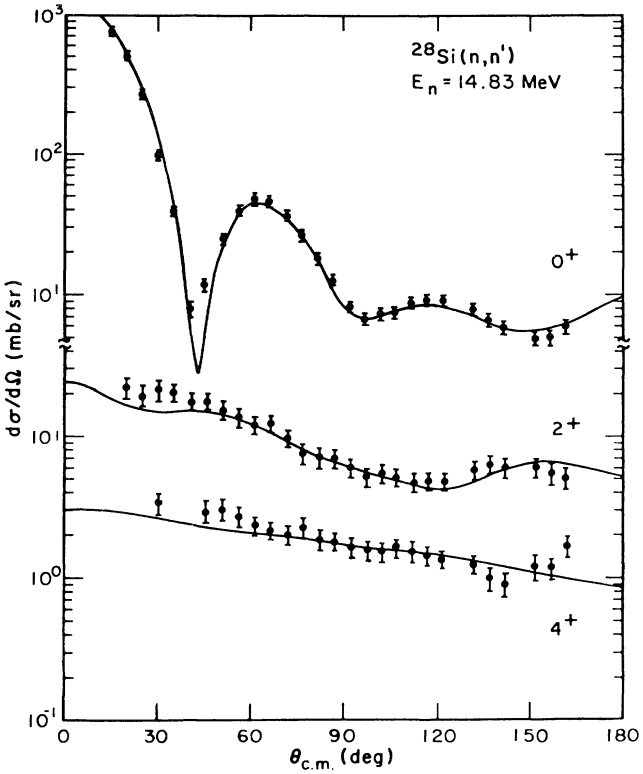

FIG. 7. Elastic and inelastic scattering differential cross sections at 14.83 MeV for ^{28}Si. The curves correspond to calculations described in the text.

were found to be negligible. The real and imaginary potential depths were taken as energy dependent and expressed as follows: $V=V_0-\alpha E$ and $W_D=W_{D0}+\alpha_D E$, where the symbol E represents the incident neutron energy. The determination of the coefficients α and α_D is described in the following. These energy-dependent potentials are suitable for evaluating precisely the compound-nucleus contribution to the elastic and inelastic scattering cross sections through transmission coefficients which had to be determined at energies between the incident neutron energy and an energy as low as possible.

The interpretation of the data followed three steps and the potential parameters were determined separately for each nucleus.

(i) A set of potential and deformation parameters was derived, in a first step, from a fit to the present elastic scattering data at 9.76 and 14.83 MeV, and also to the nonfluctuating part of the total cross section between $\simeq$0.5 and 15 MeV.[46] The fluctuations in the total cross section become important below 8–10 MeV for the three nuclei studied and can amount to about 10%. However, the smoothly varying part of the total cross section between 0.5 and 15 MeV is quite sensitive to the potential geometries and strengths as well as the deformation parameters. In this analysis the nuclei ^{24}Mg, ^{28}Si, and ^{32}S were assumed to be rigid symmetric rotors with quadrupole and hexadecapole deformations. Thus the real and imaginary potential radii are expressed, in the intrinsic coordinate system, as

$$R_i=R_{0i}A^{1/3}\left[1+\sum_{\lambda=2,4}\beta_\lambda Y_\lambda^0(\Omega')\right].$$

The coupling basis 0^+ and 2^+ was used for the calculations which were performed with a modified version[47] of Tamura's code[48] JUPITOR1. The parameter search was undertaken with the parameters of Refs. 30–32 as starting values.

(ii) The set of parameters thus determined was very close to the final set of Table I, which reflects a more complete data analysis. The deduced transmission coefficients were introduced into the statistical model code HELMAG of Lagrange and Duchemin[49] for the computation of compound-nucleus cross sections. This computer code is based on the Wolfenstein-Hauser-Feshbach formalism[50] and includes the Moldauer level width fluctuation corrections.[51] It takes explicitly into account 40 discrete levels, and higher excited levels are treated through a continuous nuclear level density.[52] The CN calculations took into account the open (n,p) and (n,α) channels as well as the open neutron channels. The possibility for interference between DI and CN mechanisms was ignored since many channels are open at 9.76 and even more at 14.83 MeV incident en-

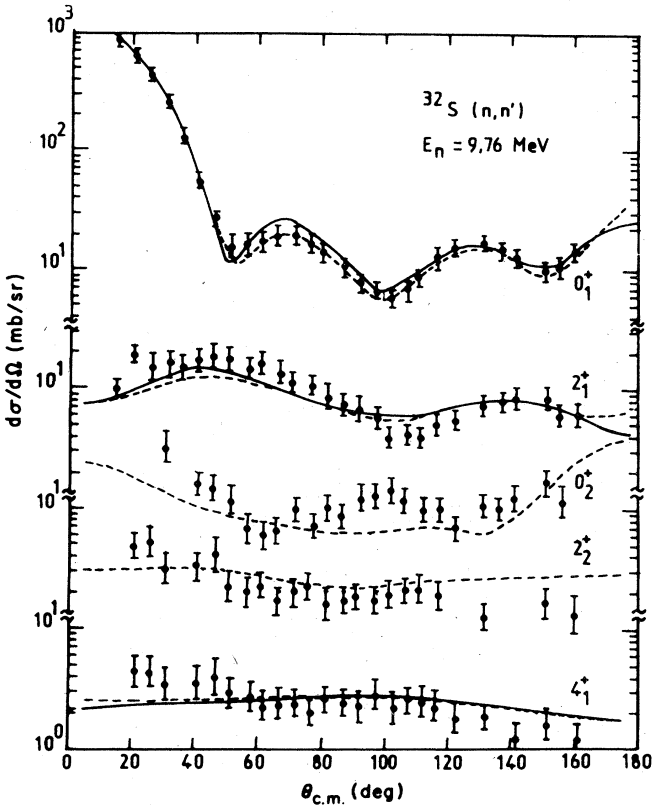

FIG. 8. Elastic and inelastic scattering differential cross sections at 9.76 MeV for ^{32}S. The full lines correspond to rotational model calculations, the dashed lines to vibrational model calculations.

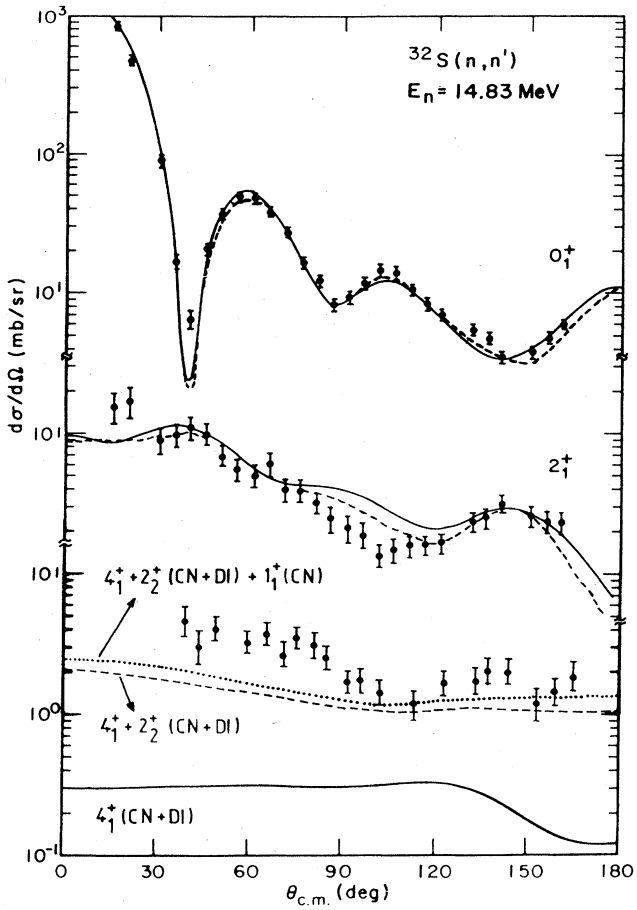

FIG. 9. Elastic and inelastic scattering differential cross sections at 14.83 MeV for ^{32}S. The full lines correspond to rotational model calculations, the dashed lines to vibrational model calculations. The dotted line corresponds to the $4_1^+ + 2_2^+$ (DI + CN) + 1^+ (CN) contributions.

ergies, thus making this effect negligible.[11]

(iii) Once the CN contribution to the cross sections was estimated and subtracted from the experimental data, the last step of the analysis consisted of fitting the "direct" elastic and inelastic scattering angular distributions at the two incident neutron energies. This yielded, for each nucleus, the final set of optical-model and deformation parameters which are listed in Table I and discussed in the following. The changes in the deformed optical potential parameters between the first and second steps were so small that we considered it to be unnecessary to reevaluate the compound-nucleus components.

A. ^{24}Mg data analysis

Three kinds of analyses were performed for ^{24}Mg. In the first analysis this nucleus was assumed to be a rigid symmetric rotor, and the coupling of the 0_1^+ (ground state), 2_1^+ (1.369 MeV), and 4_1^+ (4.123 MeV) states of the $K^\pi=0^+$ ground state (g.s.) rotational band was assumed in the coupled-channel (CC) calculations. The real and surface-imaginary potential radii were expressed as

$$R_i = R_{0i} A^{1/3}[1+\beta_2 Y_2^0(\Omega')+\beta_4 Y_4^0(\Omega')]$$

in the body fixed system. The parameters labeled S (for symmetric rotor) in Table I were thus obtained. The angular distributions calculated at 9.76- and 14.83-MeV neutron energies for the three states 0_1^+, 2_1^+, and 4_1^+ are shown as full curves in Figs. 4 and 5, respectively. They are compared to the experimental data for elastic scattering (0_1^+) and inelastic scattering to the 2_1^+ state and the unresolved 4_1^+ (4.123 MeV) $+2_2^+$ (4.239 MeV) doublet. The calculations reasonably reproduce the elastic scattering data. However, the cross sections calculated at 9.76 MeV are systematically larger than the measured values at angles beyond $\simeq 110°$ (Fig. 4). This discrepancy might be attributed to the effects of resonances existing in the total and elastic scattering cross sections around 10 MeV.[46] Calculations were performed for several different values of the β_4 deformation parameter from which it results that, in agreement with other works,[5,53,54] β_4 is very small; our best fit was obtained for $\beta_4 = 0.00 \pm 0.01$. On the other hand, the quadrupole deformation of ^{24}Mg is very large; our adopted value is $\beta_2 = +0.50 \pm 0.02$. All the calculations for the 4_1^+ state yielded values smaller than the measurements, at both neutron energies and especially at forward and backward angles (Figs. 4 and 5), which clearly indicate the importance of the 2_2^+ state excitation.

TABLE I. Neutron optical model and deformation parameters of ^{24}Mg, ^{28}Si, and ^{32}S. The potential depths and energy E are expressed in MeV, the radii and diffusionesses in fm. The symbols S, T, and V refer to the symmetric rotor, asymmetric rotor, and vibrator models, respectively. CS means coupled states.

	Nucleus:	^{24}Mg	^{28}Si	^{32}S
Real potential:	V	$54.60-0.24E$	$55.00-0.30E$	$51.70-0.18E$
	R_0	1.15	1.15	1.20
	a	0.61	0.61	0.74
Surface-imaginary potential:	$W_{(S)}$	$5.10+0.10E$	$4.90+0.12E$	$6.70+0.20E$
	$W_{(T)}$	$4.50+0.10E$		
	$W_{(V)}$			$6.20+0.20E$
	R_0	1.15	1.15	1.25
	a	0.58	0.58	0.48
SO potential:	V_{SO}	6.00	6.00	6.00
	R_0	1.15	1.15	1.20
	a	0.58	0.58	0.74
S model:	CS	$0_1^+,2_1^+,4_1^+$	$0_1^+,2_1^+,4_1^+$	$0_1^+,2_1^+,4_1^+$
	β_2	$+0.50\pm0.02$	-0.42 ± 0.02	$+0.35\pm0.02$
	β_4	0.00 ± 0.01	$+0.20\pm0.03$	-0.10 ± 0.02
T model:	CS	$0_1^+,2_1^+,4_1^+,2_2^+,3_2^+$		
	β_2	$+0.53\pm0.02$		
	γ	$21.1°\pm0.5°$		
V model:	CS			$0_1^+,2_1^+,4_1^+,0_2^+,2_2^+$
	β_2			0.35 ± 0.02

The collective low-lying states of ^{24}Mg, up to 6 MeV excitation, are believed to belong to the rotational bands built on the 0_1^+ ground state and 2_2^+ γ-vibrational state. Thus, a suitable description of the elastic and inelastic scattering from ^{24}Mg requires CC calculations extending beyond the symmetric rotor model. These calculations have been carried out in the framework of the asymmetric rotor model (ARM),[55] the rotation-vibration model (RVM),[56] and the interacting boson model (IBM).[57] The code ECIS79 of Raynal[58] was used throughout in these analyses. As for the CC calculations based on the symmetric rotor model, only the real and imaginary potentials were deformed.

For the ARM calculations, the angular dependence of the potential radius R_i has the form

$$R_i = R_{0i}A^{1/3}\left\{1+\beta_2\cos\gamma\, Y_2^0(\Omega')+\frac{\beta_2}{\sqrt{2}}\sin\gamma \times [Y_2^2(\Omega')+Y_2^{-2}(\Omega')]\right\},$$

where Ω' refers to the body-fixed system. Note that, following the conclusion of the previous discussion, no β_4 deformation had been considered here. The coupling basis used in the calculations included the 0_1^+, 2_1^+, and 4_1^+ states of the $K^\pi=0^+$ ground state rotational band and the 2_2^+ and 3_2^+ (5.236 MeV) members of the $K^\pi=2^+$ γ-vibrational band. No mixing between the two bands was

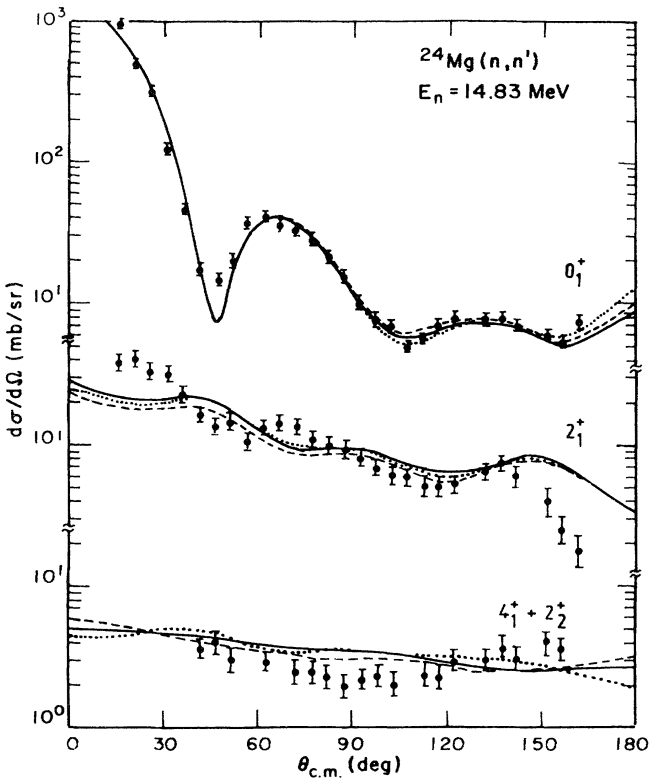

FIG. 10. Comparison of the ARM (— — —), RVM (——), and IBM (· · ·) predictions at 14.83 MeV for ^{24}Mg.

considered in these calculations. All optical-model parameters were kept identical to those of the symmetric rotor analysis, except the imaginary potential depth which had to be reduced by $\simeq 10\%$ to take into account the explicit treatment of more inelastic transitions. The parameters which best fit the experimental data are given, with the label T (T for triaxial), in Table I. The calculations are shown as dashed curves in Figs. 4 and 5. The agreement with measurements for the 0_1^+ and 2_1^+ states is as satisfactory as it was in the symmetric rotor analysis, but the fit to the data for the $4_1^+ + 2_2^+$ states is substantially improved.

For the analyses based on the RVM and IBM, the method of CC calculation used recently[59] for the description of (n,n') scattering from the ground state and excited state bands of ^{184,186}W has been adopted. The nuclear reduced matrix elements (RME's) of the collective electric-multipole operators for the target nucleus were inserted into the ECIS79 code as inputs, and it was assumed that the optical potential form factors are those calculated in the rotational model. The coupling basis used presently as well as the potential parameters (including β_2) are identical to those involved previously in the ARM calculations. The RME values associated with RVM were calculated from the formulas given in Appendix A of Ref. 59. Those associated with IBM were taken from a recent nuclear structure calculation.[60] The predictions at 14.83 MeV based on the RVM and IBM are presented in Fig. 10 as full and dotted curves, respectively. They are compared to the present measurements as well as the ARM predictions (dashed curves). The various predictions are in reasonably good agreement with the data. However, it is not possible to decide which model is the most appropriate for describing the present measurements.

B. ^{28}Si data analysis

The analysis of the n + ^{28}Si data was restricted to the elastic scattering (0^+) and the inelastic scattering to the first 2^+ (1.779 MeV) and 4^+ (4.618 MeV) excited states. Since these three states are members of the ground-state rotational band, the data were analyzed within the framework of the symmetric rotational model. The nuclear potential was assumed to have quadrupole and hexadecapole deformations. The coupling basis (0^+, 2^+, and 4^+) was used in the calculations. From the comparison of the calculated and measured cross sections it was found unambiguously that the ^{28}Si nucleus has an oblate shape with large quadrupole ($\beta_2 = -0.42$) and hexadecapole ($\beta_4 = 0.20$) deformations. This oblate shape has, indeed, been well established from many experiments using different kinds of probes[32,33,41] and from nuclear structure calculations.[2,3]

The best fits, obtained with the optical-model and deformation parameters of Table I, satisfactorily reproduce the measurements for the three states at the two neutron energies (Figs. 6 and 7). However, the calculation does not reproduce the smooth structure observed at backward angles in the experimental cross section for the 4^+ state at 9.76 MeV.

C. ^{32}S data analysis

Both rotational and vibrational models were tested for fitting the data for ^{32}S. In fact, this nucleus displays a low-lying level structure which resembles that of a spherical vibrator,[61] but its scattering properties can also be described in terms of a rigid rotor.[6,30,56]

The rotational-model analysis was carried out assuming for ^{32}S quadrupole and hexadecapole deformations. The coupling basis included the 0_1^+ (g.s.), 2_1^+ (2.230 MeV), and 4_1^+ (4.459 MeV) states which were assumed to be members of the ground-state rotational band, even though the rotational-level sequence suggests that the level at 6.410 MeV would be the 4^+ member of this band. Several calculations were performed in which the sign and magnitude of β_2 and β_4 were varied. Figures 8 and 9 show only the best fits to the data, represented by full curves; the corresponding optical-model and deformation parameters are given in Table I. These calculations indicate that the neutron scattering data for the 0_1^+, 2_1^+, and 4_1^+ states at 9.76 and 14.83 MeV do not yield a precise determination of the shape of the ^{32}S nucleus. Indeed, the elastic scattering cross sections can be equally reproduced by assuming in the CC calculations either a prolate shape ($\beta_2 = 0.35$, $\beta_4 = -0.10$) or an oblate shape ($\beta_2 = -0.35$, $\beta_4 = -0.10$) with the same set of potential parameters (Table I). However, although they do not differ greatly from the "oblate" predictions, the "prolate" ones better reproduce the measured inelastic scattering cross sections. Negative values of the β_4 parameter have been found to give much better agreement with the data; however, β_4 values from 0.00 to -0.20 yield fits of almost equal equality. Finally, the best fits were obtained for $\beta_2 = +0.35$ and $\beta_4 = -0.10$. The agreement between calculated and measured angular distributions is reasonably good at both neutron energies for the 0_1^+ and 2_1^+ states. The agreement is also fairly good for the 4_1^+ state at 9.76 MeV, but at 14.83 MeV the predicted values are much smaller than the data (Fig. 9).

In the vibrational-model analysis, the real and imaginary potentials have a radial dependence of the form

$$R_i = r_i A^{1/3}\left[1 + \sum_{\lambda\mu} \alpha_{\lambda\mu} Y_\lambda^\mu(\Omega)\right];$$

however, we used in the calculations the β_λ deformability (rms vibration) parameters which are related to the $\alpha_{\lambda\mu}$ operators. The optical potential was expanded in a Taylor series and the coupled-channel calculations were performed using the ECIS79 code.[58] The ^{32}S nucleus was assumed to have only a β_2 quadrupole vibration amplitude. The coupling basis included the ground state (0_1^+), and the one-phonon (2_1^+; 2.230 MeV) and two-phonon (0_2^+, 3.379 MeV; 2_2^+, 4.282 MeV; 4_1^+, 4.459 MeV) states. No parameter search was performed. The calculations were carried out with the potential parameters of Table I and a quadrupole vibration amplitude: $\beta_2 = 0.35$. The calculations are displayed as dashed curves in Figs. 8 and 9. The agreement with the data is comparable to that obtained earlier in the rotational-model analysis for the 0_1^+, 2_1^+, and 4_1^+ states at 9.76 MeV and for the 0_1^+ and 2_1^+ states at 14.83 MeV. The discrepancy with measured values for

TABLE II. Deformations of ^{24}Mg: experimental results. For S, see the definition in the text. CE denotes Coulomb excitation. The quadrupole deformations are obtained from $B(E2)$ values, assuming the symmetric rotor model. We use the formula

$\beta_2(1+\frac{1}{8}\sqrt{5/\pi}\beta_2)=[B(E2\uparrow)]^{1/2}(3ZR_0^2/4\pi)^{-1}$ with $R_0=1.2A^{1/3}$.

Probe	Experiment E (MeV)	Reference	Asymmetric model β_2	Asymmetric model δ_2 (fm)	Asymmetric model γ_0	Symmetric model β_2	Symmetric model δ_2 (fm)	Symmetric model β_4	Symmetric model δ_4 (fm)
(n,n′)	10–15	This work	0.53 ±0.02	1.76 ±0.18	21.1±0.5	(S) 0.51 ±0.02	1.70 ±0.17		
						0.50 ±0.02	1.66 ±0.17	0.0 ±0.01	0.0 ±0.03
	14	62				0.53			
(p,p′)	17.5	4				0.47	1.65	−0.05 ±0.08	−0.11 ±0.29
	20.3	63	0.47	1.56	21.5	(S) 0.45	1.51	−0.060	−0.20
						0.47	1.56	−0.056	−0.19
	22.5–28.5	64	0.50 −0.56	1.64 −1.84	20–22	(S)0.48–0.54	1.59–1.77		
	30.5	65	0.50	1.72	23	(S) 0.48	1.66		
	15–35	54	0.486±0.08	1.612±0.027	21	(S) 0.470±0.077	1.560±0.025	+ 0.050±0.04	+ 0.166±0.133
	40	53				0.475	1.68	−0.030	−0.11
	50	66				0.49	1.55		
	800	40	0.60	1.61	20	(S) 0.58	1.56	−0.019	−0.050
(d,d′)	26	67				0.42	1.35		
(α,α′)	17	68				0.40	1.80	0.05	
	28.5	69	0.34	1.72	35	(S) 0.33	1.68		
	42	70		1.26	24		1.23		
	104	5				(S) 0.39 ±0.01	1.36 ±0.05	−0.015±0.015	
	120	71	0.355	1.31	20.5	(S) 0.343	1.27	−0.03	−0.11
(^{16}O,^{16}O′)	25–64	72				0.413	1.56 ±0.16		
						0.470	1.60±0.25		
	47–72	26				0.30	1.19	0.0	0.0
(e,e′)	187	73				0.51	1.68		
	183–250	74				0.45	1.65	−0.06	−0.22
CE		75				0.46	1.60		

the 2_1^+ state at 14.83 MeV around 100° still remains but is less pronounced. In addition, the vibrational-model predictions are in reasonable agreement with the measurements at 9.76 MeV for the 0_2^+ and 2_2^+ states. The comparison between the combined contributions calculated for the 4_1^+ and 2_2^+ states (dashed curve) and the measurements at 14.83 MeV for the unresolved 4_1^+, 2_2^+, and 1_1^+ (4.695 MeV) states (Fig. 9) shows a disagreement. Although uncertainties in the calculated cross sections may account for part of the discrepancy, a strong excitation of the 1^+ state cannot be excluded. Differences still remain between the measured data and the calculations, which include the DI and CN contributions to the 4_1^+ and 2_2^+ states as well as the CN contribution to the 1^+ state (Fig. 9), suggesting that this unnatural parity state might be excited by direct interaction from the ground state via a spin-flip mechanism or by a two-step process, as was recently suggested for the scattering of protons from the 3^+ (5.236 MeV) state of ^{24}Mg.[54]

V. DISCUSSION

A large amount of experimental data on nuclear deformation in the $2s$-$1d$ shell exists to which our results can be compared. However, the different studies cannot be directly compared among themselves since the determination of nuclear shape strongly depends upon the nature of the nuclear probe, the model for the target nucleus (rotor, vibrator, etc.), the interaction formalism (coupled channels, distorted wave Born approximation, etc.) used for the data analysis, the model space (coupling basis) employed in the calculations, and the choice of the optical-model parameters. It has been suggested by Blair[34] that the data would be better compared on the basis of the deformation lengths $\delta_\lambda=\beta_\lambda R$ (R: radius of the real potential) rather than the deformation parameters. Also, Mackintosh has shown that comparing the multipole moments of the charge or nuclear potential distributions would lead to better agreement among the results, since

TABLE III. Deformations of ^{28}Si: experimental results. CE denotes Coulomb excitation. The quadrupole deformations are derived from $B(E2)$ values assuming the symmetric rotor model. We use the formula

$$\beta_2\left(1+\tfrac{1}{8}\sqrt{5/\pi}\beta_2\right)=[B(E2\uparrow)]^{1/2}(3ZR_0^2/4\pi)^{-1} \text{ with } R_0=1.2A^{1/3}\,.$$

Probe	Experiment E (MeV)	Method	Reference	β_2	δ_2 (fm)	β_4	δ_4 (fm)
(n,n′)	10–15	CC	This work	−0.42±0.02	−1.47±0.10	+0.20±0.05	+0.70±0.10
	9.8	CC	30	−0.48	−1.67		
	10	CC	32	−0.48	−1.68	0.15	0.52
	13.9	CC	76	+0.41	+1.41		
	14.1	CC	31	+0.39	+1.50		
	14.1	CC	33	−0.39	−1.42		
	14.0	DWBA	62	0.40±0.04	1.52±0.15		
	14.1	DWBA	62	0.43	1.64		
	14.7	DWBA	28	0.40±0.02	1.54±0.10		
(p,p′)	17.5	DWBA	77	0.55±0.02	2.10		
	17.5	CC	4	−0.34	−1.24	+0.25	+0.91
	20.3	CC	78	−0.55	−2.00	+0.33	+1.20
	30.3	CC	79	+0.41	+1.68		
	30.3	CC	6	−0.40	−1.35	+0.10	+0.34
	20.25	CC	80	−0.40	−1.40	+0.15	+0.52
	26.40	CC	41	−0.37	−1.32	+0.15	+0.53
(d,d′)	12.8	CC	81	+0.446			
	52	DWBA	82	0.41	1.56		
(α,α′)	28.4	DWBA	83	0.29	1.46		
	28	CC	84	+0.36			
	104	CC	5	−0.32±0.01	−1.34	+0.08±0.01	+0.34
(^{16}O,^{16}O′)	45–63	CC	27	−0.34	−1.35		
(e,e′)	183–250		74	−0.39	−1.31	+0.10	+0.34
(CE)			85	−0.39	−1.42		

these quantities are much less model dependent.[35] In this work we compare our values of the deformation parameters and deformation lengths to the results of other experiments.

Experimental deformation values for ^{24}Mg are presented in Table II. Only the data which were obtained from CC calculations have been considered. They have been obtained assuming either the symmetric rotor (S) or the triaxial rotor (T) models. The β_λ and δ_λ values extracted from the two kinds of calculations may not be comparable. However, since both models should yield the same value of the reduced electric quadrupole transition probability $B(E2; 0_1^+ \rightarrow 2_1^+)$, one can derive from the β_2,γ parameters for the asymmetric rotor a symmetric-rotor equivalent quadrupole deformation β_2^*, given by the relation[55]

$$\beta_2^* = \beta_2^T \left\{ \frac{1}{2} \left\{ 1 + \frac{3 - 2\sin^2(3\gamma)}{[9 - 8\sin^2(3\gamma)]^{1/2}} \right\} \right\}^{1/2} .$$

The values thus obtained for β_2^* and δ_2^*, labeled S in Table II, can be directly compared to the β_2,δ_2 values for the symmetric rotor.

Our quadrupole deformation data from both the S and T calculations are found to be in good agreement with the other neutron and proton data as well as the electromagnetic data, the β_2 (β_2^*) values ranging between 0.45 and 0.53 with an average value of $\bar{\beta}_2 = 0.50$ and the δ_2 (δ_2^*) values between 1.51 and 1.70 with an average value of $\bar{\delta}_2 = 1.62$. On the other hand, the results for composite particles yield substantially smaller values for β_2 and occasionally δ_2. However, the prolate form of ^{24}Mg is evident from all measurements. The values found for the hexadecapole deformation are very small, with a negative sign, but they often vanish within the limits of error, in agreement with our determination of $\beta_4 = 0.00 \pm 0.01$.

The nuclear shape of ^{28}Si has been investigated in a number of neutron scattering experiments. The deformation parameters derived in these studies are listed in Table III together with the results of other works. All data presented in this table were determined within the framework of the symmetric rotational model. Some of the analyses were carried out using the DWBA formalism which is known to be insensitive to the sign of the multipole deformations. On the other hand, the coupled-channel analyses indicate for ^{28}Si either an oblate or a prolate shape (Table III). As already mentioned, the oblate shape is, however, clearly shown by Coulomb excitation (CE) measurements[85] and by the most recent neutron and proton studies,[32,33,41] as well as by the results of this work. Moreover, Hartree-Fock and Hartree-Fock-Bogolyubov calculations suggest an oblate shape for the ground state rotational band.[2,3]

Looking at the neutron data in Table III, we observe good agreement for the magnitude of both β_2 and δ_2, since

TABLE IV. Deformations of ^{32}S: experimental results. CE denotes Coulomb excitation. The quadrupole deformations are derived from $B(E2)$ values assuming the symmetric rotor model. We use the formula

$\beta_2(1+\frac{1}{8}\sqrt{5/\pi}\beta_2) = [B(E2\uparrow)]^{1/2}(3ZR_0^2/4\pi)^{-1}$ with $R_0 = 1.2A^{1/3}$.

Probe	Experiment E (MeV)	Method	Reference	Vibrational model β_2	δ_2 (fm)	Rotational model β_2	δ_2 (fm)	β_4	δ_4 (fm)
(n,n')	10–15	CC	This work	+0.35±0.03	+1.33±0.13	+0.35 ±0.03	1.33±0.13	−0.10±0.02	−0.38±0.08
	6	CC	86	0.36					
	8	CC	87	0.37					
	9.8	CC	30	0.31	1.19	+0.30	+1.14		
						−0.33	−1.26		
	14.0	DWBA	62			0.40			
	14.1	DWBA	62			0.32			
	13.9	CC	42	0.30	1.22	+0.28	+1.09		
	21.5	CC	88	0.30	1.20	−0.34	−1.36		
(p,p')	17.5	CC	89			+0.30	+1.15	−0.27	−1.04
	24.5	CC	90	0.29		+0.29			
	30.3	CC	89			+0.30	+1.04	−0.15	−0.52
	30.3	CC	6	0.30	1.14				
	15.35	CC	91	0.28	1.04				
	15.5–41	CC	92	0.29	1.06				
(d,d')	18	DWBA	61			0.30			
	18	CC	61	0.286					
	18	DWBA	82			0.27			
(α,α')	104	CC	93	0.216		0.211			
CE			85			0.30	1.20		

$|\beta_n^{n,n'}|$ in all cases lies between 0.38 and 0.48 and $|\delta_2^{n,n'}|$ lies between 1.38 and 1.68. The mean values, $|\overline{\beta_2^{n,n'}}|=0.42$ and $|\overline{\delta_2^{n,n'}}|=1.52$, are very close to our results. These $\beta_2^{n,n'}$ values are comparable to those found for proton scattering ($|\beta_2^{p,p'}|=0.43$; $|\delta_2^{p,p'}|=1.52$) and to the (d,d'), (e,e'), and Coulomb excitation (CE) results. In contrast, the results of (α,α') and (^{16}O, ^{16}O') experiments are also somewhat smaller for this nucleus.

The hexadecapole deformation of ^{28}Si has been less investigated. The obtained results are somewhat scattered and no systematic trend is observed (see Table III). However, except for one measurement,[32] they definitely indicate a positive sign and a large value for β_4 in agreement with most of the nuclear structure calculations.[2,3]

Deformation data for ^{32}S are shown in Table IV, which includes values obtained from calculations based on the symmetric rotational model and on the vibrational model. It is evident from this table that rotational-model analyses of the inelastic scattering to the low-lying collective states cannot distinguish between the prolate shape and the oblate shape of ^{32}S; nevertheless, the majority of data slightly favor a prolate shape for this nucleus. It is clear, on the other hand, that the vibrationlike character of this nucleus becomes apparent from the investigation of the 0_2^+ (3.778 MeV), 2_2^+ (4.282 MeV), and 4_1^+ (4.459 MeV) states.

Table IV shows that the β_2 and δ_2 parameters determined from different kinds of measurements are generally in good agreement with each other, except for the (α,α') data of Schweimer *et al.*[93] which are again smaller. Our rotational-model parameters are close to the mean values for the neutron data ($\overline{\beta_2^{n,n'}}=0.34$; $\overline{\delta_2^{n,n'}}=1.24$), but slightly larger than the proton mean values ($\overline{\beta_2^{p,p'}}=0.30$; $\overline{\delta_2^{p,p'}}=1.10$). The same features are observed for the vibrational-model results for which $\overline{\beta_2^{n,n'}}=0.32$, $\overline{\delta_2^{n,n'}}=1.25$ and $\overline{\beta_2^{p,p'}}=0.29$, $\overline{\delta_2^{p,p'}}=1.08$. Because too few values of the hexadecapole deformation parameter are available, no statement about this parameter can be made; nevertheless, the measurements shown in Table IV indicate unambiguously a negative sign for β_4.

VI. SUMMARY AND CONCLUSIONS

Nuclear shapes and deformations in the $2s$-$1d$ shell have been investigated through fast neutron scattering on ^{24}Mg, ^{28}Si, and ^{32}S. Accurately measured cross sections for elastic and inelastic scattering at the incident energies of 9.76 and 14.83 MeV have been analyzed using several surface excitation models.

No attempt was made to describe the scattering properties of the three nuclei with a single scattering potential since they have quite different collective behaviors. Both the direct-interaction and compound-nucleus mechanisms were considered in the analyses; the potential parameter searches were based on the present results and on total cross section data over a wide energy range in order to improve the consistency of the extracted optical-model parameters and the confidence in the predicted cross sections.

The nuclear potential deformations were determined using the coupled-channel formalism. No energy dependence of the deformation parameters was found for any of the three nuclei. From the analyses of the inelastic scattering to the excited states of its ground state band, the ^{24}Mg nucleus exhibits unambiguously the shape of a prolate rotor with a large quadrupole deformation and a small hexadecapole deformation. However, to reproduce correctly the inelastic scattering to the states belonging to the γ band, it is necessary to assume that ^{24}Mg is either a triaxial rotor or an axially symmetric deformed vibrator. The permanent oblate deformation of the ground states of ^{28}Si, which has been well established in recent studies, is confirmed in the present work. On the other hand, it is hard to specify the actual detailed shape of ^{32}S. The elastic scattering and inelastic scattering to the low-lying collective states can be described as well by the rotational model as by the vibrational model. For the rotational model, the experimental data favor a prolate shape. However, the vibrational model yields a more consistent description of the collective properties of ^{32}S.

The quadrupole deformations and deformation lengths of the three nuclei extracted in the present work are in agreement with other data from (n,n'), (p,p'), (d,d'), and charge distribution measurements. But these results exhibit systematic differences with those of α particles and other composite particle measurements. If these differences were to remain in the nuclear multipole moments, which are nearly reaction-model independent, they would suggest that these heavier projectiles tend to sample differently the nuclear volume, as was recently suggested in a study of the ^{238}U deformations.[94]

The excellent agreement found in the neutron and proton β_2 and δ_2 values leads to a tentative explanation. The interaction of neutrons with these $N=Z$ nuclei is identical to the interaction of protons, if one does not take into account the Coulomb force. Thus, because the neutron and proton density distributions are similar in these light nuclei,[95] the neutrons and protons feel the same deformed nuclear potential. In this context, it is not surprising to find also that the electromagnetic studies yield β_2 and δ_2 values close to those obtained in (n,n') and (p,p') measurements.

ACKNOWLEDGMENTS

The authors are indebted to J. Chardine and A. Virdis for their generous cooperation in the data reduction. They wish to express their gratitude to M. Girod for useful discussions and for giving them the results of Hartree-Fock-Bogolyubov calculations prior to publication.

*Permanent address: Institut des Sciences Nucléaires, 53 Avenue des Martyrs, 38026 Grenoble Cedex, France.

†Permanent address: Lawrence Livermore National Laboratory, University of California, P.O. Box 808, Livermore, CA 94550.

[1]O. Haüsser, T. K. Alexander, A. B. McDonald, and W. T. Diamond, Nucl. Phys. **A175**, 593 (1971); D. Pelte, O. Haüsser, T. K. Alexander, and H. C. Evans, Can. J. Phys. **47**, 1929 (1969); K. Nakai, J. L. Quebert, F. S. Stephens, and R. M. Diamond, Phys. Rev. Lett. **24**, 903 (1970); D. Schwalm, A. Bamberger, P. G. Bizetti, B. Povh, G. A. Engelbertink, J. W. Olness, and E. K. Warburton, Nucl. Phys. **A192**, 449 (1972); A. Olin, O. Haüsser, T. K. Alexander, A. J. Ferguson, and W. Witthunn, *ibid.* **A221**, 555 (1974); G. Dannhauser, J. de Boer, R. Lutter, F. Ries, and H. Bohn, Z. Phys. A **300**, 71 (1981).

[2]G. Ripka, in *Advances in Nuclear Physics*, edited by M. Beranger and E. Vogt (Plenum, New York, 1968), Vol. I; H. C. Lee and R. Y. Cusson, Ann. Phys. (Paris) **72**, 353 (1972); M. Girod and B. Grammaticos, Phys. Rev. C **27**, 2317 (1983).

[3]H. G. Benson and B. H. Flowers, Nucl. Phys. **A126**, 305 (1969); B. Casteland and J. C. Parikh, Phys. Rev. C **1**, 990 (1970); A. L. Goodman, G. L. Struble, J. Bar-Touv, and H. Goswami, *ibid.* **2**, 380 (1970); D. Goss, *ibid.* **2**, 1168 (1970).

[4]R. de Swiniarski, C. Glashausser, D. L. Hendrie, J. Sherman, A. D. Bacher, and E. A. McClatchie, Phys. Rev. Lett. **23**, 317 (1969).

[5]H. Rebel, G. W. Schweimer, G. Schatz, J. Specht, R. Lohken, G. Hauser, D. Habs, and H. Klewe-Nebenius, Nucl. Phys. **A182**, 145 (1972).

[6]R. de Swiniarski, F. G. Resmini, D. L. Hendrie, and A. D. Bacher, Nucl. Phys. **A261**, 111 (1976).

[7]G. Blanpied, B. Ritchie, M. Barlett, G. Hoffmann, J. McGill, E. Milner, C. Glasshausser, K. Jones, S. Nanda, R. de Swiniarksi, M. Franey, M. Gazzaly, and B. Wildenthal, in *Proceedings of the International Conference on Nuclear Structure, Amsterdam, 1982*, edited by A. van der Woude and B. J. Verhaar (ICONS, Amsterdam, 1982), Vol. I, p. 171.

[8]D. L. Hendrie, N. K. Glendenning, B. G. Harvey, O. N. Jarvis, H. H. Duhm, J. Saudinos, and J. Mahoney, Phys. Lett. **26B**, 127 (1968).

[9]T. Kruse, W. Makofske, H. Ogata, W. Savin, M. Slagowitz, M. Williams, and P. Stoler, Nucl. Phys. **A169**, 177 (1971).

[10]I. Y. Lee, J. X. Saladin, J. Holden, J. O'Brien, C. Baktash, C. Bemis, Jr., P. H. Stelson, F. K. McGowan, W. T. Milner, J. L. C. Ford, Jr., R. L. Robinson, and W. Tuttle, Phys. Rev. C **12**, 1483 (1975).

[11]J. P. Delaroche, G. Haouat, J. Lachkar, Y. Patin, J. Sigaud, and J. Chardine, Phys. Rev. C **23**, 136 (1981).

[12]J. M. Moss, Y. D. Terrien, R. M. Lombard, C. Brassard, J. M. Loiseaux, and F. G. Resmini, Phys. Rev. Lett. **26**, 1488 (1971).

[13]H. Kind, J. E. Finck, G. M. Crawley, J. A. Nolen, Jr., and R. M. Ronningen, Phys. Rev. C **20**, 2084 (1979).

[14]I. Brissaud, G. Berrier-Ronsin, J. Cameron, R. Frascaria, J. Kalifa, G. Bagieu, and R. de Swiniarski, Z. Phys. A **293**, 1 (1979).

[15]R. M. Ronningen, R. C. Melin, J. A. Nolen, Jr., G. M. Crawley, and C. E. Bemis, Jr., Phys. Rev. Lett. **47**, 635 (1981).

[16]G. Haouat, J. Lachkar, Ch. Lagrange, J. Jary, J. Sigaud, and Y. Patin, Nucl. Sci. Eng. **81**, 491 (1982).

[17]L. F. Hansen, I. D. Proctor, D. W. Heikkinen, and V. A. Madsen, Phys. Rev. C **25**, 189 (1982).

[18]P. David, J. Debrus, H. Essen, F. Lübke, H. Mommsen, R. Schoenmackers, W. Soyez, H. V. Geramb, and E. F. Hefter, Z. Phys. A **278**, 281 (1976).

[19]A. H. Shaw and J. S. Greenberg, Phys. Rev. C **10**, 263 (1974).

[20]M. T. McEllistrem, R. E. Shamu, J. Lachkar, G. Haouat, Ch. Lagrange, Y. Patin, J. Sigaud, and F. Cocu, Phys. Rev. C **15**, 927 (1977).

[21]G. Haouat, J. Lackkar, Ch. Lagrange, M. T. McEllistrem, Y. Patin, R. E. Shamu, and J. Sigaud, Phys. Rev. C **20**, 78 (1979).

[22]J. W. Frickey, K. A. Eberhard, and R. H. Davis, Phys. Rev. C **4**, 434 (1971).

[23]R. J. Peterson and F. E. Cecil, Nucl. Phys. **A297**, 10 (1978).

[24]K. W. Kemper, D. S. Haynes, and N. R. Fletcher, Phys. Rev. C **4**, 108 (1971).

[25]E. Fabrici, S. Micheletti, M. Pignanelli, F. G. Resmini, R. De Leo, G. D'Erasmo, and A. Pantaleo, Phys. Rev. C **21**, 844 (1980).

[26]K. Siwek-Wilczynska, J. Wilczynski, and P. R. Christensen, Nucl. Phys. **A229**, 461 (1974).

[27]A. Dudek-Ellis, V. Shkolnik, and D. Dehnhard, Phys. Rev. C **18**, 1039 (1978).

[28]J. Höhn, H. Pose, D. Seeliger, and R. Reif, Nucl. Phys. **A134**, 289 (1969).

[29]J. D. Brandenberger, A. Mittler, and M. T. McEllistrem, Nucl. Phys. **A196**, 65 (1972).

[30]A. W. Obst and J. L. Weil, Phys. Rev. C **7**, 1076 (1973).

[31]S. Kliczewski and Z. Lewandowski, Nucl. Phys. **A304**, 269 (1978).

[32]W. Pils, D. Schmidt, D. Seeliger, and T. Streil, in Proceedings of the IXth International Symposium on the Interaction of Fast Neutrons with Nuclei, Gaussig, 1979, edited by D. Seeliger and S. Unholzer, Zentralinstitut für Kernforschung Report 410 (1980); M. Adel-Fawzy, D. Schmidt, D. Seeliger, and T. Streil, *ibid.* p. 60.

[33]J. Böttcher, H. Blank, E. Finckh, C. Forstner, W. Jaumann, G. Schall, H. Scheuring, U. Schneidereit, K. S. Tauber, A. Weipert, W. Tornow, and E. Woye, J. Phys. G **9**, L65 (1983).

[34]D. L. Hendrie, Phys. Rev. Lett. **31**, 478 (1973); J. S. Blair, in *Direct Interactions and Nuclear Reaction Mechanisms*, edited by E. Clementel and C. Villi (Gordon and Breach, New York, 1963), p. 669.

[35]R. S. Mackintosh, Nucl. Phys. **A266**, 379 (1976).

[36]V. R. Brown and V. A. Madsen, Phys. Rev. C **11**, 1298 (1975); V. A. Madsen, V. R. Brown, and J. D. Anderson, Phys. Rev. Lett. **34**, 1398 (1975); V. A. Madsen, V. R. Brown, and J. D. Anderson, Phys. Rev. C **12**, 1205 (1975).

[37]R. S. Mackintosh, Nucl. Phys. **A209**, 91 (1973); **A210**, 245 (1973).

[38]H. Rebel and G. W. Schweimer, Z. Phys. A **262**, 59 (1973).

[39]R. S. Mackintosh, Nucl. Phys. **A280**, 86 (1977).

[40]G. Blanpied, N. M. Hintz, G. S. Kyle, J. W. Palm, R. Liljestrand, M. Barlett, C. Harvey, G. W. Hoffmann, L. Ray, and D. G. Madland, Phys. Rev. C **20**, 1490 (1979).

[41]R. De Leo, G. D'Erasmo, A. Pantaleo, G. Pasquariello, G. Viesti, M. Pignanelli, and H. V. Geramb, Phys. Rev. C **19**, 646 (1979).

[42]R. De Leo, G. D'Erasmo, E. M. Fiore, A. Panteleo, and G. Pasquariello, Phys. Rev. C **22**, 337 (1980).

[43]A. Virdis, Commissariat á l'Energie Atomique Report CEA-R-5144, 1981.

[44]H. Liskien and A. Paulsen, Nucl. Data Tables **11**, 569 (1973).

[45]W. E. Kinney, Nucl. Instrum. Methods **83**, 15 (1970).

[46]J. Stehn, M. Goldberg, B. Magurno, and R. Weiner-Chasman, Neutron Cross Sections, Brookhaven National Laboratory

Report BNL 325, 1964, 2nd ed., Suppl. No. 2.
[47]Ch. Lagrange and N. Mondon, Centre d'Etudes de Limeil Internal Report, 1973 (unpublished).
[48]T. Tamura, Oak Ridge National Laboratory Report No. ORNL-4152, 1967.
[49]Ch. Lagrange and B. Duchemin, Statistical model code HELMAG, 1974 (unpublished).
[50]L. Wolfenstein, Phys. Rev. **82**, 690 (1951); W. Hauser and H. Feshbach, *ibid.* **87**, 366 (1952).
[51]P. A. Moldauer, Phys. Rev. **123**, 968 (1961); **129**, 754 (1963).
[52]A. Gilbert and A. G. Cameron, Can. J. Phys. **43**, 1446 (1965).
[53]B. Zwieglinski, G. M. Crawley, H. Nann, and J. A. Nolen, Jr., Phys. Rev. C **17**, 872 (1978).
[54]R. De Leo, G. D'Erasmo, E. M. Fiore, A. Panteleo, M. Pignanelli, and H. V. Geramb, Phys. Rev. C **20**, 13 (1979).
[55]A. S. Davydov and G. F. Filippov, Nucl. Phys. **8**, 237 (1958).
[56]A. Faessler, W. Greiner, and R. K. Sheline, Nucl. Phys. **70**, 33 (1965).
[57]F. Iachello, in *Interacting Bosons in Nuclear Physics,* edited by F. Iachello (Plenum, New York, 1979), p. 1.
[58]J. Raynal, coupled-channel code ECIS79, 1979 (unpublished).
[59]J. P. Delaroche, Phys. Rev. C **26**, 1899 (1982).
[60]H. Clement, in *Interacting Bose-Fermi Systems in Nuclei,* edited by F. Iachello (Plenum, New York, 1981), p. 31.
[61]M. C. Mermaz, C. A. Whitten, Jr., and B. A. Bromley, Phys. Rev. **187**, 1466 (1969).
[62]P. H. Stelson, R. L. Robinson, H. J. Kim, J. Rapaport, and G. R. Satchler, Nucl. Phys. **68**, 97 (1965); R. L. Clarke and W. G. Cross, *ibid.* **53**, 177 (1964).
[63]R. M. Lombard, J. L. Escudie, and M. Soyeur, Phys. Rev. C **18**, 42 (1978).
[64]I. Lovas, M. Rogge, U. Schwinn, P. Turek, and D. Ingham, Nucl. Phys. **A286**, 12 (1977).
[65]J. Eenmaa, R. K. Cole, C. N. Waddell, H. S. Sandhu, and R. R. Dittman, Nucl. Phys. **A218**, 125 (1974).
[66]A. A. Rush and N. K. Ganguly, Nucl. Phys. **A117**, 101 (1968).
[67]H. Tjin, A. Djie, K. Mulder, F. Udo, A. Groeneveld, L. Koerts, A. Hill, and P. Hodgson, Nucl. Phys. **A106**, 85 (1968).
[68]K. A. Eberhard and D. Robson, Phys. Rev. C **3**, 149 (1971).
[69]T. Tamura, Nucl. Phys. **73**, 241 (1965).
[70]J. Vincent, E. Boschitz, and J. Priest, Phys. Lett. **25B**, 81 (1967).
[71]K. Van de Borg, M. Harakeh, and B. Nilsson, Nucl. Phys. **A325**, 31 (1979).
[72]W. Mittig, P. Charles, S. M. Lee, I. Badawy, B. Berthier, B. Fernandez, and J. Gastebois, Nucl. Phys. **A233**, 48 (1974).
[73]R. Helm, Phys. Rev. **104**, 1466 (1956).
[74]Y. Horikawa, Y. Yorizuka, A. Nakada, S. Mitsunobu, Y. Kojima, and M. Kimura, Phys. Lett. **36B**, 9 (1971).
[75]B. Zwieglinski, G. M. Crawley, W. Chung, H. Nann, and J. A. Nolen, Jr., Phys. Rev. C **18**, 1228 (1978).
[76]R. De Leo, G. D'Erasmo, E. Fiore, A. Panteleo, and M. Pignanelli, Phys. Rev. C **20**, 1244 (1979).
[77]G. M. Crawley and G. T. Garvey, Phys. Rev. **160**, 981 (1967).
[78]A. Blair, C. Glashausser, R. de Swiniarksi, J. Goudergues, R. Lombard, B. Mayer, J. Thirion, and P. Vaganov, Phys. Rev. C **1**, 444 (1970).
[79]R. K. Cole, C. N. Waddell, R. Dittman, and H. Sandhu, Nucl. Phys. **75**, 241 (1966).
[80]R. de Swiniarski, H. E. Conzett, C. R. Lamontagne, B. Frois, and R. J. Slobodrian, Can. J. Phys. **51**, 1293 (1973).
[81]H. Niewodniczanski, J. Nurzynski, A. Strzalowski, J. Wilcynski, J. R. Rook, and P. E. Hodgson, Nucl. Phys. **55**, 386 (1964).
[82]F. Hinterberger, G. Mairle, U. Schmidt-Rohr, G. Wagner, and P. Turek, Nucl. Phys. **A115**, 570 (1968).
[83]J. Kokame, K. Fukunaga, and H. Nakamura, Nucl. Phys. **A108**, 655 (1968).
[84]J. Kokame, K. Fukunaga, N. Inoue, and H. Nakamura, Phys. Lett. **8**, 342 (1964).
[85]G. Ball, O. Hausser, T. Alexander, W. Davies, J. Forster, I. Mitchell, J. Beene, D. Horn, and W. McLatchie, Nucl. Phys. **A349**, 271 (1980).
[86]J. Martin, D. T. Stewart, and W. H. Currie, Nucl. Phys. **A113**, 564 (1968).
[87]S. Tanaka, K. Tsukada, M. Maruyama, and Y. Tomita, in Proceedings of the International Conference on Nuclear Data for Reactors, Helsinki, 1970 (International Atomic Energy Agency, Vienna, 1970), Vol. 2, p. 317.
[88]Y. Yamanouti, Nucl. Phys. **A283**, 23 (1977).
[89]R. de Swiniarski and D. L. Pham, Lett. Nuovo Cimento **16**, 391 (1976).
[90]R. Lombard and J. Raynal, Phys. Rev. Lett. **31**, 1015 (1973); R. Lombard, H. Kamitsubo, J. Raynal, and J. Gosset, C. R. Acad. Sci. **B274**, 761 (1972).
[91]R. de Leo, G. D'Erasmo, E. Flore, G. Guarino, and A. Pantaleo, Nuovo Cimento **59A**, 101 (1980).
[92]R. De Leo, G. D'Erasmo, E. Fiore, G. Guarino, A. Pantaleo, S. Micheletti, M. Pignanelli, and L. Serafini, Phys. Rev. C **25**, 107 (1982).
[93]G. Schweimer, H. Rebel, G. Nowicki, G. Hauser, and R. Lohken, Phys. Lett. **39B**, 627 (1972).
[94]P. Quentin, I. Brissaud, and R. de Swiniarski, Z. Phys. A **298**, 37 (1980).
[95]M. Girod (private communication).